ESCUELA DE CONSTRUCCIÓN CIVIL
FACULTAD DE INGENIERÍA

Revista de la Construcción
Journal of Construction

Research Article

Effect of waste oyster shell powder as additive on properties and sulfate attack resistance of mortar

Yu-Wen Liu [1], Shih-Wei Cho [2], *, Pou-Gang Chiou [3]

[1] Department of Civil and Water Resources Engineering, National Chiayi University, Chiayi (Taiwan); yuwen@mail.ncyu.edu.tw
[2] Department of Civil Engineering and Engineering Management, National Quemoy University, Kinmen (Taiwan); swcho@nqu.edu.tw
[3] Department of Civil and Water Resources Engineering, National Chiayi University, Chiayi (Taiwan);
*Corresponding author: swcho@nqu.edu.tw (C. Shih-Wei)

Received: 29.09.2022; **Accepted:** 17.12.2023; **Published:** 31.08.2024

Citation: Liu, Y.W., Cho, S. W., and Chiou, P.G. (2024). Effect of waste oyster shell powder as additive on properties and sulfate attack resistance of mortar. Revista de la Construcción. Journal of Construction, 23(2), 164-176. https://doi.org/10.7764/RDLC.23.2.164

Abstract: In this study, the waste oyster shell powder was added in mix design to investigate the properties, sulfate attack resistance and sulfide bacterial of concrete. Add 0%, 1%, 3%, 6% and 9% oyster shell powder to the concrete to replace part of the sand. The study conducted flow tests, compressive strength tests, sulfate corrosion resistance and antibacterial tests. From the results, it was found that adding oyster shell powder improved the resistance to sulfate corrosion and anti-bacterial properties and became more effective as the substitution ratio increased. In addition, the sulfate attack resistance and antibacterial have a linear relationship of mortar with oyster shell powders.

Keywords: sulfate attack resistance, waste oyster shell powder, anti-sulfide bacteria effect, mortar.

1. Introduction

Microbially induced corrosion (MIC) caused by sulfide bacteria is the most severe durability problem associated with cementitious materials in underground structures such as concrete sewer pipes (Roghanian and Banthia, 2019; Lavigne et al., 2015; Wu et al., 2019) design regulations stipulate a minimum covered depth of 50 mm for reinforced concrete sewer pipes. The soil in Taiwan is slightly acidic (approximate pH of 5.5–6.5); moreover, the soil contains decaying organic matter that, upon fermentation, produces hydrogen sulfide gas, which is easily oxidized into sulfuric acid by Sulfide bacteria (i.e., Thio-bacillus) (Wu et al., 2019). Furthermore, sulfates in sewage are easily reduced by Sulfide bacteria into hydrogen sulfide, which is then oxidized into sulfuric acid. The detrimental effect of sulfuric acid on concrete lies in its formation of calcium sulfate with cement hydrates, which reacts with $CaO \cdot Al_2O_3$ to form ettringite ($3CaO \cdot Al_2O_3 \cdot 3CaSO4 \cdot 32H_2O$). The formation of ettringite, used as an expansion agent in engineering, can engender a solid-phase volume expansion of approximately 700% (Chang and Choi, 2020; Wang et al., 2020; Grengg et al., 2017). Because the hydration reaction rate of concrete decreases when ettringite is formed, its volume is fixed and the rate of change is extremely low; thus, no space is available for ettringite to expand. Consequently, the expansion force causes the concrete to crack, in turn causing the rebar to come into contact with the electrolyte-filled liquid, which oxidizes and corrodes the rebar and results in damage to the sewer pipes. This process is called MIC damage (Roghanian and Banthia, 2019; Chang and Choi, 2020; Tanyildizi, 2024).

Sewer pipes are located in environments laden with hydrogen sulfide; therefore, inhibiting the growth of sulfide bacteria on the concrete surface can help avoid the conversion of hydrogen sulfide into sulfuric acid, thereby extending the service life of reinforced concrete. Previously, the contents of C_2S and C_4AF in cement were increased to produce cement with resistance to sulfate corrosion, such as Type II and Type V cement (Grengg et al., 2018; American Concrete Association, 2014; Silva et.al.,2024). However, because the aforementioned types of cement are not extensively used, cement plants must set up separate production lines to manufacture them, which contributes to the difficulty of purchasing related products on the market and to their high costs. Moreover, if a relatively high proportion of C_4AF is added to cement, the compressive strength of the resulting cement is lower than that of Type I cement, which thus increases the unit cement content used in concrete.

Daczko et al. (1997) used silica fume and an organic corrosion-inhibiting admixture to prevent MIC. Chang and Choi (2020) developed mortar with rapid-hardening cement and polyvinyl acetate (PVA) resin powder to repair concrete pipes damaged by MIC and reported that the repair mortar with PVA powder could improve sulfur resistance. Torii and Kawamura (1994) studied the sulfate attack resistance of mortar composed of fly ash and silica fume and reported that the pozzolans could consume the Ca $(OH)_2$ in the mortar to minimize sulfate attack. Nnadi and Lizarazo-Marriaga (2013) studied the antibacterial capacity of concrete with fly ash. Akyuncu et al. (2017) also studied the sulfur resistance of concrete with lass F and Class C fly ashes, and concluded that increasing the amount of fly ash added would help the concrete's sulfur resistance. All of the aforementioned studies have changed the mixture composition to reduce the amount of ettringite produced by the reaction between sulfuric acid and $CaO \cdot Al_2O_3$. By contrast, other studies have employed antimicrobial agents (biocides) to prevent the reaction of Sulfide bacteria and hydrogen sulfide gas. For example, Monteny et al. (2001) studied the MIC resistance of four polymer cement concrete specimens and indicated that the concrete specimen with the styrene–acrylic ester polymer had a higher MIC resistance. On the basis of the aforementioned studies, the aim of the present study was to develop and add a new high-activity bactericidal material to concrete and evaluate the effectiveness of this material in improving MIC resistance. This material is expected to facilitate the realization of the principle of waste recycling.

Because of the increasing popularity of the circular economy in recent years, materials that were originally regarded as waste are being reused in concrete to improve its properties, leading to a design trend for new concrete ratios. Accordingly, this study added processed and ground powder of discarded oyster shells to concrete and explored the MIC resistance of the resulting concrete. Because Taiwan is an island country, the aquaculture industry established along the southwest coast has made considerable contributions to Taiwan's economic development. Oysters constitute the primary source of income for the aquaculture industry in the central and southern coastal areas of Taiwan. In 2019, more than 6 million tons of oyster meat is produced in global (Botta et al., 2020), resulting in a considerable amount of discarded oyster shells. Because of their low recycling rate and low added value, most of the shells are discarded directly without treatment, which severely affects environmental sanitation and causes environmental problems. Therefore, the disposal of discarded oyster shells is a crucial topic that merits attention. Approximately 95% of an oyster shell is composed of calcium carbonate; therefore, some researchers have attempted to add ground oyster shell powder to concrete as a substitute for cement (Naqi et al., 2020; Chen et al., 2019; Lavanya et al., 2024). Naqi et al. (2020) studied the effect of oyster shell powder as an additive on the properties of high-volume slag cement; the test results revealed that the workability and strength of the resulting concrete decreased with increasing oyster shell powder content, rendering such powder incapable of replacing the most expensive component (cement) of concrete. Chen et al. (2019) used crash oyster shells as an alternative to river sand and reported that the strength and durability of the resulting concrete increased with curing time. Naqi et al. (2024) conducts research using oyster shell powder modified with silane coupling agents to replace part of the cement in concrete. It was found that at a substitution rate of 1.5%, the modified oyster shell powder increased the compressive strength and durability of the concrete. However, no related study investigated the MIC resistance of oyster shell powder in cementitious materials.

In other research fields, Mori and Takahashi (1998) found the manufacture of ceramic filter materials and discovered that oyster shell powder had a strong antibacterial effect after high-temperature sintering Sawai et al. (2006) observed that high-temperature sintering could convert oyster shells into a calcium oxide (CaO) structure that can generate active oxygen under the induction of hydroxyl groups. Lian et al. (2021) noted that the oyster shells decomposed into CaO at 900 °C. Wu et al. (2011) reported that pure hydroxyapatite was obtained after sintering the 1-h oyster shells powder at 1000 °C for 1 h. Active oxygen consists of superoxide anions (O_2^-), hydrogen peroxide radicals (HOO^-), and hydrogen peroxide (H_2O_2), all of which

possess oxidizing capacities. Daniels et al. (2010) noted that the superoxide air anions react with bioaerosols in the air and convert them into charged bioaerosols to induce a bacterial removal or sterilization function. The application of air anions includes the elimination of indoor microorganisms, odors, and volatile organic pollutants. Shargawi et al. (1999) reported that air anions can sterilize certain non-aerosol microorganisms. Accordingly, in the present study, oyster shells were calcined, ground into powder, and added to mortar to examine their influence on the mechanical properties as well as MIC resistance of mortar. Its novelty is the discovery of the possibility of adding waste oyster shell powder to concrete to resist sulfate bacteria. It can be helpful for sewer projects or foundation projects.

2. Materials and methods

In order to avoid the interactive effect of changes in paste composition on the addition of oyster shell powder. In this study, oyster shell powder was added to the mortar by replacing part of the fine aggregate, different oyster shell powder additions—0%, 1%,3%, 6%, and 9% (S0, S1, S3, S6, and S9) of the weight of the substituted fine aggregate—served as the main variable. A polycarboxylate-based superplasticizer with 40.22% solid contents and a density of 1.07 g/cm^3 was used for improvement workability. The defoamer with 0.02 wt.% tributyl phosphate and a density of 1.1 g/cm^3 was also used to reduce the bubble during mixing. To increase the durability and reduce carbon emissions of the mortar and minimize the use of cement, fly ash and blast-furnace slag were used to replace part of the cement in the mortar. The total substitution amount was 30%, with the ratio of fly ash to blast-furnace slag being maintained at 3:7(refer to previous researches (Aiken et al., 2020; Shah and Huseien, 2020)). Portland Type 1 cement, blast-furnace slag and Class F fly ash were employed. The specific gravity of cement, fly ash, and blast-furnace slag were 3.15, 2.2, and 2.82, respectively. The fine aggregate consisted of natural river sand with a specific gravity of 2.64, a water absorption rate of 1.33%, and a fineness modulus of 2.98. Figure 1 showed that the waste oyster shells before sintering. To prepare the oyster shell powder, oyster shells were ground after being calcined at 1000°C for 1 hour and subsequently cooled (refer to previous researches (Lian et al., 2021; Wu et al., 2011)). The waste oyster shells after sintering and grinding was showed in Figure 2.

Figure 1. The waste oyster shells before sintering.

Figure 2. The waste oyster shells after sintering and grinding.

The absorption rate and specific gravity of the powder were 1.65% and 2.67, respectively. The Blaine surface area of cement, fly ash, blast-furnace slag, and oyster shell powder were 3654 cm^2/g, 4782 cm^2/g, 6282 cm^2/g, and 5109 cm^2/g. The powder composition and particle size distribution were presented in Table 1 and Figure 3, respectively. Table 2 listed the mix designs of mortar.

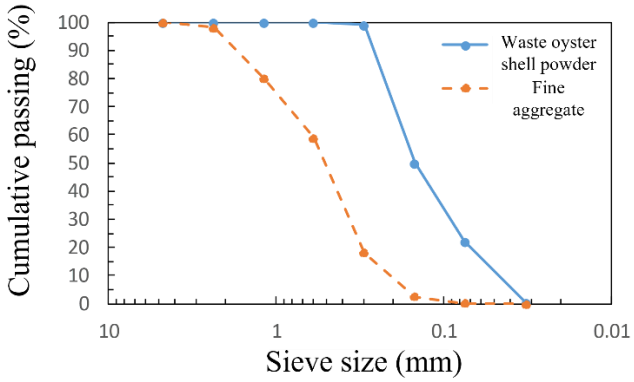

Figure 3. Particle size distribution of fine aggregate and waste oyster shell powder.

Table 1. Chemical composition and source of oyster shell powder, cement, blast-furnace slag, and fly ash.

Chemical composition	Oyster shell powder	Cement	Blast-furnace slag	Fly ash
Material source	Taiwan coast	Asia cement Co., Ltd.	CHC resources corp	Taiwan power company
		Chemical composition (unit: %)		
CaO	54.30	63.56	41.16	4.8
SiO_2	2.17	21.04	33.42	56.00
Na_2O	1.51	0.32	0.10	0.31
Al_2O_3	1.10	5.46	13.35	24.80
MgO	0.75	2.56	7.76	1.48
SO_3	0.45	2.01	0.61	0.36
Fe_2O_3	0.33	2.98	0.21	5.30
Ignition loss	37.62	1.38	0.30	5.78
Others	1.77	0.69	3.09	1.16

Table 2. Chemical composition and source of oyster shell powder, cement, blast-furnace slag, and fly ash.

Trial no.	Water	Cement	Blast-furnace Slag	Fly ash	Oyster shell powder	Sand	Super-plasticizer	Defoaming agent
S0	180	360	108	46	0	1679	8	0
S1	180	360	108	46	17	1663	8	5
S3	180	360	108	46	51	1629	8	5
S6	180	360	108	46	102	1579	8	5
S9	180	360	108	46	153	1528	8	5

Each mortar was hardened and cured in water to the required age, after which relevant tests were conducted. The tests consisted of a flow test based on ASTM C1437 and a compressive strength test based on ASTM C109; the specimen of compressive strength test in each curing age were three 50 × 50 × 50 mm3 cube specimens and conducted on specimens cured for 7, 28, and 56 days. For the results of this study to be applicable to sewers, a sodium sulfate drying–immersion cycle test and an anti-sulfide bacterial test were conducted; the test methods are described in the following paragraphs.

Due to the long test time (15 weeks required) and insufficient equipment, this study did not use ASTM C1012 as the test method for sulfate resistance evaluation. The alternative method was the sodium sulfate drying–immersion cycle test. The test

was performed in accordance with the ASTM C88 soundness test method for coarse aggregates. Both test methods used sodium sulfate as the main component of the dipping solution, but ASTM C88 used a saturated solution (35.6%), which had a higher concentration than ASTM C1012 (5%). And used the dry and immersion cycle as a degradation mechanism. A 28-day-old 50 × 50× 50 mm^3 mortar cube specimen was placed in an oven at 110°C ± 5°C for 24 h, after which the specimen's dried weight was measured. Subsequently, the specimen was immersed in a 23°C ± 2°C saturated sodium sulfate solution for 24 hours and then dried in the oven for another 24 hours, after which its weight was measured again. These 48-hour test was repeated for five cycles in the same way as the ASTM C88 method.

The anti-sulfide bacterial test was conducted in accordance with ASTM E2149. In this test, the ability of the mortar to inhibit the growth of Thiobacillus trioxidanes was primarily assessed. The experiment was divided into four parts: preparation of culture medium, growth of bacterial culture, immersion of the specimen in the bacterial liquid, and measurement of the concentration of bacteria attached to the specimen. Table 3 presents the culture medium used to produce T. trioxidanes. T. trioxidanes (its bacterial strain information is listed in Table 4). T. trioxidanes was produce in the culture medium for 10–14 days, after which a polymerase chain reaction test (PCR) was performed to confirm whether the bacteria were successfully cultured. Subsequently, the optical density (OD) value of the solution was obtained using an OD spectrophotometer (Figure 4) to measure the amount of bacterial in solution.

Table 3. Culture medium composition.

Composition	Content
$(NH_4)_2SO_4$	2 g
KNO_3	3 g
KH_2PO_4	3 g
$MgCl_2 \cdot 6H2O$	0.5 g
$CaCl_2 \cdot 2H2O$	0.25 g
$FeSO_4 \cdot 7H_2O$	0.0 1g
$Na_2S_2O_3 \cdot 5H_2O$	5 g
$Na_2MoO_4 \cdot 2H_2O$	0.3 mg
Yeast extract	0.1 g
Sulfur	1 g
Bromophenol blue	10 mg
Distilled water	1 L

In OD measurement using a spectrophotometer, light of a specific wavelength is incident on the water sample in the sample tube and then enters a photoelectric tube, where the light energy is converted into an electrical signal to obtain the difference in light energy absorbed between the sample and the blank water sample. A 50 × 50 × 10 mm3 test piece was immersed in the bacterial solution for 3 and 7 days (Figure 5). After reaching the immersion days, take out the immersion solution and place it in a 3.5mL quartz cuvette and measure it with a spectrophotometer.

Table 4. Strain information of T. trioxidanes.

Item	Information
BCRC number	80191
Organism	Thiobacillus thiooxidans
Characterization	Taxonomy of B1714
Growth conditions	30 °C medium ID: 828
Biosafety level	1

Figure 4. Optical density spectrophotometer.

Figure 5. Test piece immersed in the bacterial solution.

3. Experimental results and analysis

3.1. *Flow test*

Flow test was measured in accordance with ASTM C230. It was the increase in expansion diameter after the fluidity test. Expressed as a percentage of the original base diameter. Figure 6 shows the relationship between flow results and the amount of oyster shell powder added. The flow result of the oyster shell powder mortar was lower than that of the reference S0 mortar, and test results decreased with the addition of oyster shell powder. The flow result of the S9 mortar decreased by 11.5% compared to the S0 mortar without the addition of oyster shell powder. From Figure 3, it was found that the particle of oyster shell powder was much finer than the fine aggregate. When the addition ratio increases, the specific surface area in contact with the paste increased, causing the water to be agglomerated and reducing fluidity.

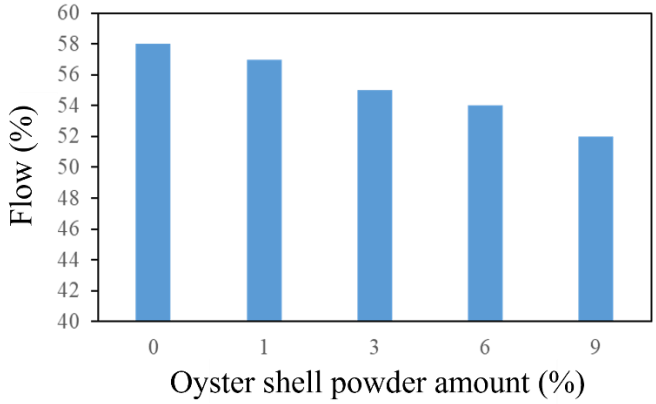

Figure 6. Influence of oyster shell powder content on mortar fluidity.

3.2. *Compressive strength test*

Figure 7 displays the compressive strength development curve for the oyster shell powder mortar. The compressive strengths of S0 mortar were 41.5, 54.5, and 59.1 MPa on days 7, 28, and 56, respectively. Its strength development on 7 and 28 days reached 70% and 92% of that on 56 days, respectively. The compressive strength of the oyster shell powder mortar on 7 days was almost the same as that of the reference group (41 MPa), but its compressive strength on 28 and 56 days were lower than that of the reference group. The compressive strength of oyster shell powder mortar was lower than S0 mortar by 1.8% to 5.7% at 28-day curing age, and 6.6% to 9.3% lower than S0 mortar at 56-day curing age. From the literature (Naqi et al., 2020) and Table 1, it is found that although oyster shell powder has a large amount of CaO, the content of SiO_2 and Al_2O_3 was too low to produce hydration reaction.

Therefore, the effects of oyster shell powder on its compressive strength were its fine particle size and high specific surface area. The finer particles filled the intervening space between coarse and fine aggregates, leading to positive benefits. However, a higher specific surface area was increasing the interface area between the paste and the aggregate, which was a negative effect. In Figure 7, the compressive strength of oyster shell powder mortar is lower than S0, and the influence of specific surface area could be found. Figure 8 compares the relationship between the compressive strength and the amount of oyster shell powder added. The standard deviation error bars ware plotted at the center of the chart in Figure 6. The standard deviation of compressive strength ranged from 0.55 to 1.11 MPa. It was found that the compressive strength of S6 mortar was slightly higher than other mortars containing oyster shell power, but it was still lower than S0 mortar.

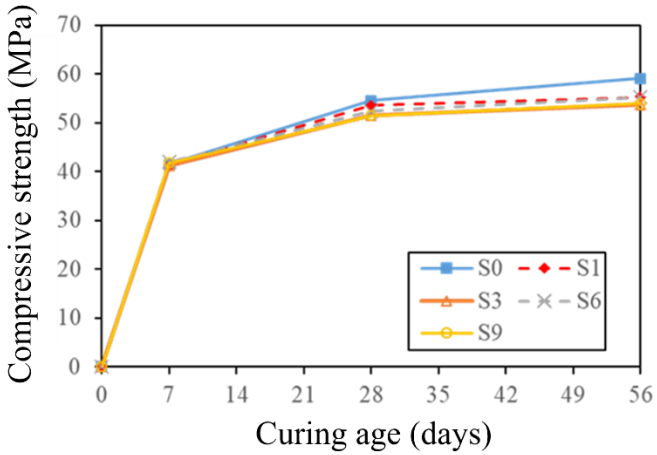

Figure 7. Compressive strength development of oyster shell powder mortar.

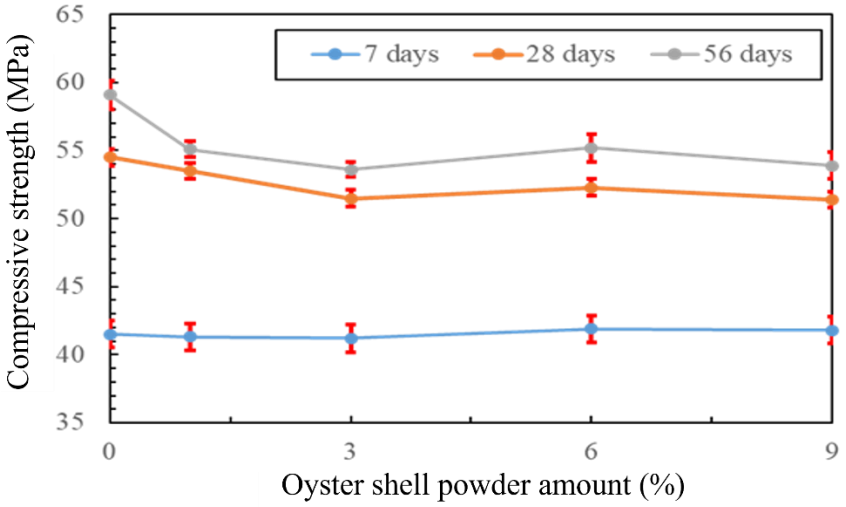

Figure 8. Effect of oyster shell powder content on compressive strength of oyster shell powder mortar. Error bar is the standard deviation.

3.3. *Sodium sulfate drying–immersion cycle test*

The effect of the oyster shell powder content on the sulfate attack resistance of the mortar is presented in Figure 9. The weight loss rate of the reference specimen after five cycles was 4.9%. The weight loss rate of the oyster shell powder mortar after five cycles was lower than that of the reference specimen by 2.7%–4.0%. It was obvious from Figure 9. that the mortar added with oyster shell powder had the ability to resist sulfate. Figure 10 shows the relationship between the 28-day compressive strength results and the weight loss of the specimen. It can be found from the figure that the two results have a roughly linear relationship. When the weight loss of the specimen increases, the compressive strength also increases. Although increasing the amount of oyster shell replacement will reduce the compressive strength, but the weight loss of the specimen is reduced because the oyster shell power itself has the effect of sulfate resistance.

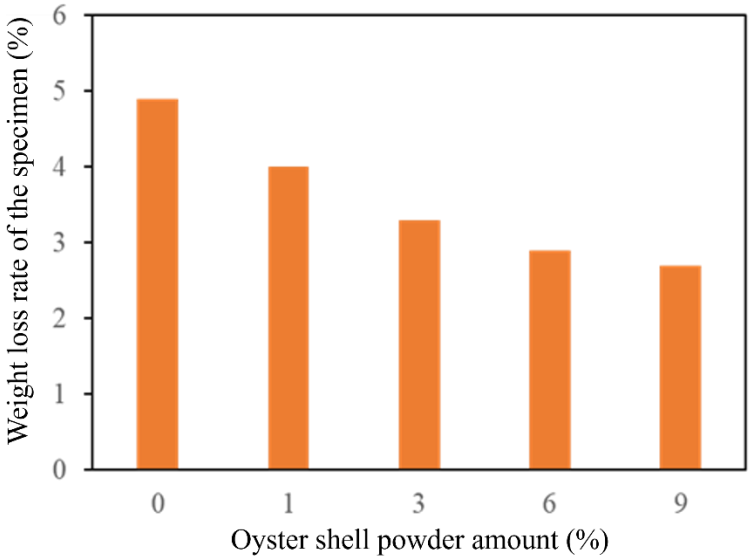

Figure 9. Weight loss rate of oyster shell power mortar after the sodium sulfate drying–immersion cycle test.

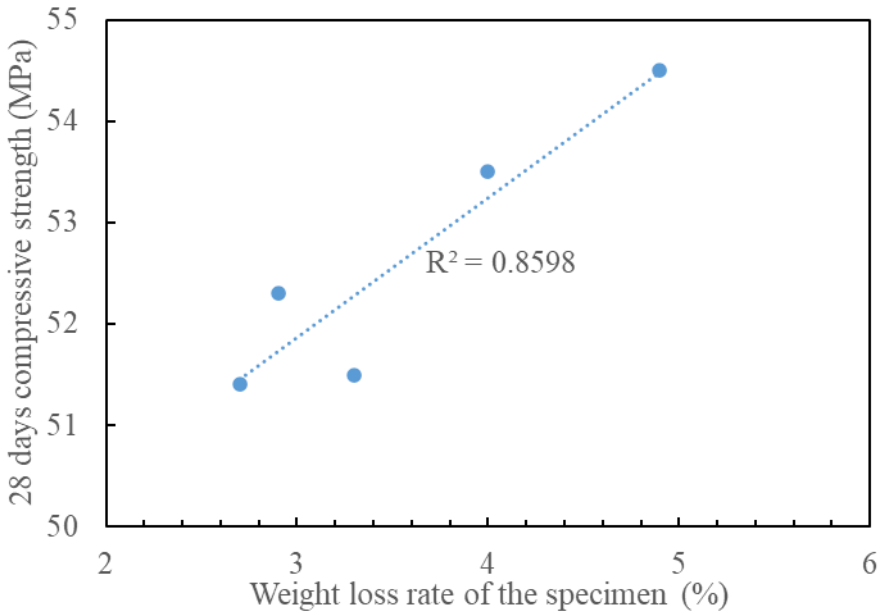

Figure 10. The relationship between the 28-day compressive strength results and the weight loss of the specimen.

3.4. *Antibacterial test*

Microorganism-induced corrosion of sewer pipes decreases their durability. The objective of this study was to improve the antibacterial capacity of sewer pipes and enhance their durability by adding recycled materials with anti-sulfide bacterial effects. Figure 11 illustrates the antibacterial test results. Under normal culture conditions, the OD value of the liquid without the test piece (blank test) was 0.15 on day 3, 0.17 on day 6, and 0.22 on day 10.

The reference mixture (S0) exhibited a slower increase in OD on day 6 compared with that of the blank group. The OD value on day 10 was also lower than that of the blank group, indicating that the composition of the reference group had a slight inhibitory effect on the growth of sulfide bacteria. When the oyster shell powder mortar specimen was added, the OD value showed an increasing trend in the first 3 days of the experiment. However, after 3 days, the OD value decreased gradually. The test results obtained on 10 days were all lower than those obtained for the S0 mortar. This demonstrates that the addition of the oyster shell powder improved the anti-sulfide bacterial effects.

Figure 12 displays the measured OD and pH values on day 10. The pH of the blank test was 1.75, which is close to the pH range of sulfuric acid. When the reference mortar test pieces were added to the bacterial solution, the pH value increased to 6.75, and the pH value of the oyster shell powder mortar test pieces increased to 7.6. A comparison of the OD values revealed that the oyster shell powder reduced the concentration of the bacterial solution converted to sulfuric acid, thereby increasing the pH value of the bacterial solution. On day 10, the OD value of the oyster shell powder mortar test piece was lower than that of the reference specimen. And the OD value decreased with the oyster shell powder content. In this study, the sulfate resistance test of mortar containing oyster shell powder was carried out with reference to ASTM C88 test procedure. The mortar sample was also put into the sulfur bacteria, and the bactericidal effect of the sulfur bacteria was calculated by a spectrophotometer. Figure 13 compares the results of the two experiments for the same variables. There is a good linear relationship between the two experimental values. Compared with the complicated test procedures of the antibacterial test, the sulfate resistance test based on the weight loss rate is relatively simple. Therefore, it is suggested that the sulfate resistance test can be used as a rapid evaluation test method in the future.

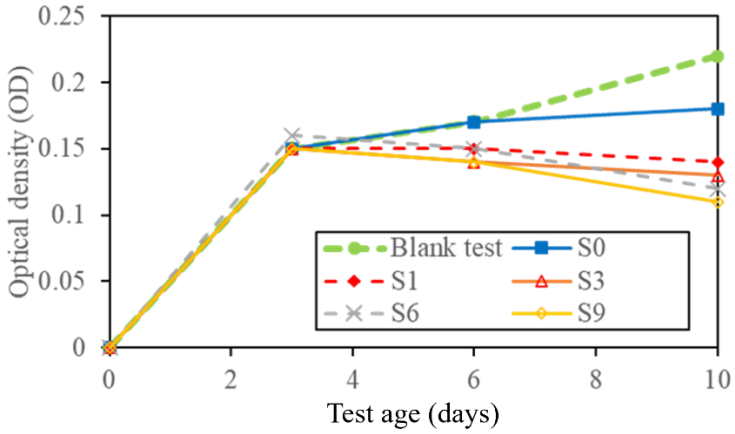

Figure 11. Antibacterial test results for mortar species.

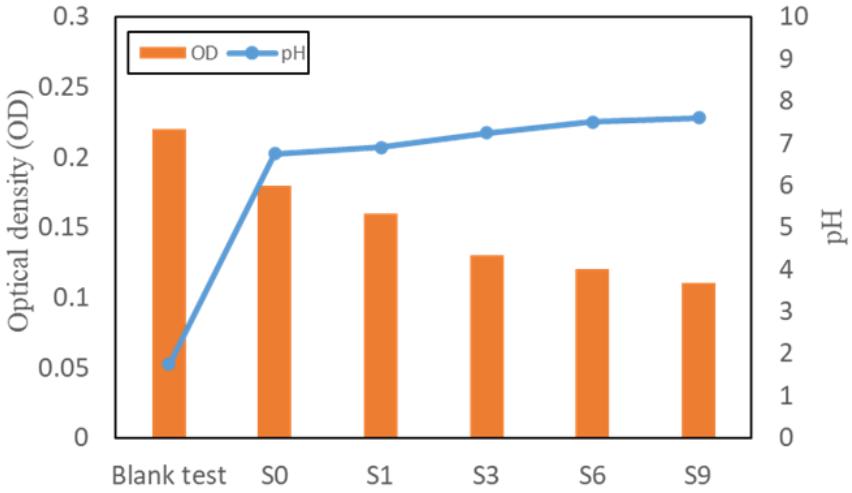

Figure 12. OD and pH values of mortar specimens on 10 days.

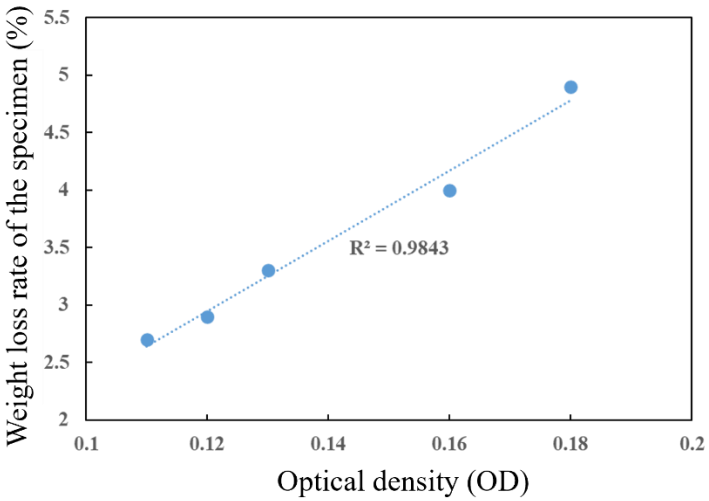

Figure 13. Relationship between weight loss rate and optical density of mortar with oyster shell powder.

4. Conclusions and comments

This study investigated the engineering properties, sulfuric acid attack resistance of mortar containing oyster shell powder. On the basis of the test results, the following conclusions can be drawn:

1. When the oyster shell powder was added to the mortar, the flow of the mortar decreased with the addition ratio increases. The flow result of the mortar with 9% oyster shell powder decreased by 11.5% compared to the reference mortar.
2. The compressive strength of oyster shell powder mortar was lower than reference mortar by 1.8% to 5.7% at 28-day curing age, and 6.6% to 9.3% lower than reference mortar at 56-day curing age.
3. The weight loss rate of the oyster shell powder mortar after Sodium sulfate drying–immersion cycle test was lower than that of the reference specimen by 2.7%–4.0%.
4. Mortar with oyster shell powder had better results in resisting sulfate attack.in antibacterial test, the OD value of the oyster shell powder mortar were all lower than those obtained for the reference mortar.
5. The relationship between the test results of the sodium sulfate drying–immersion cycle test and antibacterial test has a good linear relationship.
6. Future research work will study the resistance to mold after oyster shell powder is added to concrete.

Author contributions:

Yu-Wen Liu: Conceptualization, Project administration, Review and editing. **Shih-Wei Cho**: Conceptualization, Writing original draft. **Pou-Gang Chiou:** Conceptualization, Experimental testing.

Funding:

This work was supported by the Ministry of Science and Technology [MOST-106-2221-E-415-005, 2017].

Conflicts of interest:

The author would like to declare that the author does not have any potential conflict of interest regarding this research.

References

Aiken, T. A., Kwasny, J., Sha, W., and Tong, K. T. (2020). Mechanical and Durability Properties of Alkali-Activated Fly Ash Concrete with Increasing Slag content. Construction and Building Materials. 251, 124330.

Akyuncu, V., Uysal, M., Tanyildizi, H., and Sumer, M. (2018). Modeling the Weight and Length Changes of the Concrete Exposed to Sulfate Using Artificial Neural Network. Revista de la Construcción. Journal of Construction, 17(3), 337–353.

American Concrete Association (2014). Precast Concrete Pipe Durability, Concrete Pipe Information CPInfo. https://www.concretepipe.org/wpcontent/uploads/CP InfoDurability072116.pdf.

Botta, R., Asche, F., Borsum, J. S., and Camp, E., (2020). A Review of Global Oyster Aquaculture Production and Consumption. Marine Policy. 117, 103952.

Chang, H. B., and Choi, Y. C. (2020). Accelerated Performance Evaluation of Repair Mortars for Concrete Sewer Pipes Subjected to Sulfuric Acid Attack. Journal of Materials Research and Technology. 9, 13635-13645.

Chen, D., Zhang, P., Pan, T., and Liao, Y. (2019). Evaluation of the Eco-Friendly Crushed Waste Oyster Shell Mortars Containing Supplementary Cementitious materials. Journal of Cleaner Production. 237, 117811.

Daniels C., Merrifield D., Boothroyd D., Davies S., and Factor, J. (2010). Effect of Dietary Bacillus Spp. and Mannan Oligosaccharides (MOS) on European Lobster (Homarus gammarus L.) Larvae Growth Performance, Gut Morphology and Gut Microbiota. Aquaculture. 304, 49-57.

Daczko, J. A., Johnson, D. A., and Arney, S. L. (1997). Decreasing Concrete Sewer Pipe Degradation Using Admixtures. Materials Performance. 36, 51-56.

Fernando Silva, Y., Delvasto, S., Valencia, W., and Araya-Letelier, G. (2024). Performance of Self-Compacting Concrete with Residue of Masonry and Recycled Aggregate under Sulfate Attack. Journal of Materials in Civil Engineering, 36(1), 04023491.

Grengg, C., Mittermayr, F., Koraimann, G., Konrad, F., Szabó, M., Demeny, A. and Dietzel, M. (2017)., The Decisive Role of Acidophilic Bacteria in Concrete Sewer Networks: A New Model for Fast Progressing Microbial Concrete Corrosion. Cement and Concrete Research. 101, 93-101.

Grengg, C., Mittermayr, F., Ukrainczyk, N., Koraimann, G., Kienesberger, S., and Dietzel, M. (2018), Advances in Concrete Materials for Sewer Systems Affected by Microbial Induced Concrete Corrosion: A Review. Water Research. 134, 341-352.

Lavanya, M. R., Johnpaul, V., Balasundaram, N., and Venkatesan, G. (2024). Potential use of silane-modified oyster shell powder in hydrophobic concrete. Materials Research Express, 11(5), 055508.

Lavigne, M. P., Bertron, A., Auer, L., Hernandez-Raquet, G., Foussard, J., Escadeillas, G., Cockx, A., and Paul, E. (2015). An Innovative Approach to Reproduce the Biodeterioration of Industrial Cementitious Products in a Sewer Environment. Part I: Test Design. Cement and Concrete Research. 73, 246-256.

Lian, W., Li, H., Yang, J., Joseph, S., Bian, R., Liu, X., Zheng, J., Drosos, M., Zhang, X., Li, L., Shan, S., and Pan, G. (2021). Influence of Pyrolysis Temperature on the Cadmium and Lead Removal Behavior of Biochar Derived from Oyster Shell Waste. Bioresource Technology Reports. 15, 100709.

Monteny, J., De Belie, N., Vincke, E., Verstraete, W., and Taerwe, L. (2001). Chemical and Microbiological Tests to Simulate Sulfuric Acid Corrosion of Polymer-Modified Concrete, Cement and Concrete Research. 31, 1359-1365.

Mori, K., and Takahashi, K. (1998). Bactericidal Effects on Escherichia Coli of the Water Treated with New Ceramics Manufactured by a Combination of Burned Oyster Shells and Natural Zeolite. Mizushorigijutu (Water Purification and Liquid Waters Treatment). 39, 1-7.

Nnadi, E. O., and Lizarazo-Marriaga, J. (2013). Acid Corrosion of Plain and Reinforced Concrete Sewage Systems. Journal of Materials in Civil Engineering. 25, 1353-1356.

Naqi, A., Siddique, S., Kim, H. K., and Jang, J. G. (2020). Examining the Potential of Calcined Oystershell Waste as Additive in High Volume Slag Cement. Construction and Building Materials. 230, 116973.

Roghanian, N.,and Banthia N. (2019). Development of a Sustainable Coating and Repair Material to Prevent Bio-Corrosion in Concrete Sewer and Waste-Water Pipes. Cement and Concrete Composites, 100, 99-107.

Sawai, J., and Shiga, H. (2006). Kinetic Analysis of the Antifungal Activity of Heated Scallop-Shell Powder Against Trichophyton and its Possible Application to the Treatment of Dermatophytosis. Biocontrol Science. 11, 125–128.

Shah, K.W., and Huseien G.F. (2020). Bond Strength Performance of Ceramic, Fly Ash and GBFS Ternary Wastes Combined Alkali-Activated Mortars Exposed to Aggressive Environments, Construction and Building Materials. 251, 119088.

Shargawi, J. M., Theaker, E. D., Drucker, D. B., MacFarlane, T., and Duxbury, A. J. (1999). Sensitivity of Candida Albicans to Negative Air Ion Streams. Journal of Applied Microbiology. 87, 889–897.

Tanyildizi, H. (2024). Durability of Concrete Exposed to Combined Freeze-thaw, Sulfate, and Acid Attacks after Two Years. Revista de la Construcción. Journal of Construction, 22(1), 102–121. https://doi.org/10.7764/RDLC.22.1.102

Torii, K., and Kawamura, M. (1994). Effects of Fly Ash and Silica Fume on the Resistance of Mortar to Sulfuric Acid and Sulfate Attack, Cement and Concrete Research. 24, 361-370.

Wang, T., Wu, K., Kan, L., and Wu, M. (2020). Current Understanding on Microbiologically Induced Corrosion of Concrete in Sewer Structures: a Review of the Evaluation Methods and Mitigation Measures. Construction and Building Materials. 247, 118539.

Wu, S. C., Hsu, H. C., Wu, Y. N., and Ho, W. F. (2011). Hydroxyapatite Synthesized from Oyster Shell Powders by Ball milling and Heat Treatment. Materials Characterization. 62, 1180-1187.

Wu, S. C., Hsu, H. C., Hsu, S. K., Tseng, C. P., and Ho, W. F. (2017). Preparation and Characterization of Hydroxyapatite Synthesized from Oyster Shell Powders. Advanced Powder Technology. 28, 1154-1158.

Wu, L., Hu, C., and Liu, W. V. (2018). The Sustainability of Concrete in Sewer Tunnel—A Narrative Review of Acid Corrosion in the City of Edmonton, Canada. Sustainability, 10, 517.

Wu, M., Wang, T., and Kan, L. (2020). Microbiologically Induced Corrosion of Concrete in Sewer Structures: A Review of the Mechanisms and Phenomena. Construction and Building Materials. 239, 117813.